Bond Behavior of GFRP-reinforced lightweight concrete beams

Hala Mamdouh[1], Ahmed H. Ali [2], Nehal M. Ayash[3], Kareem A. M.[4]

[1]Associate Professor, Civil Engineering Department, Faculty of Engineering at Mataria, Helwan University,11718, Cairo, Egypt.

[2]Corresponding author. Associate Professor of Civil Engineering, Helwan University, Cairo, Egypt.

[3]Corresponding author. Assistant Professor, Civil Engineering Department, Faculty of Engineering at Mataria, Helwan University,11718, Cairo, Egypt.

[4]Demonstrator, Civil Engineering Department, Faculty of Engineering at Mataria, Helwan University,11718, Cairo, Egypt

Abstract: **More study is required to better understand the flexural behaviour and cracking performance of fiber-reinforced polymer (FRP) bars used in lightweight concrete (LWC) beams because there is a paucity of experimental research in this field. This article describes an experimental investigation that evaluated the flexural behaviour, cracking capability, and bond-dependent (Kb) properties of beams made of lightweight concrete. There are three thin concrete beams in all (one of them reinforced with steel bars as a reference beam and the other beams reinforced with GFR bars) measured 150 mm wide x 300 mm deep x 2000 mm long were constructed and tested up to failure in four-point bending over a clear span of 1800 mm. The test parameters were: (a) reinforcement type (Steel bars and GFRP bars), and (b) concrete cover (20 mm and 35 mm). The test results included information on the cracking behaviour, deflection, crack width, reinforcing strain, flexural capacity, and mechanism of failure. The experiment's findings showed that the GFRP-reinforced beams behaved linearly to cracking until concrete crushing caused them to fail. Additionally, the predicted moment capacities of the GFRP beams were computed using the strain-compatibility approach in the design standards. The outcomes showed that the experimental results and predictions had a good degree of agreement. According to the analysis of the kb factor, recommended Kb values for smooth GFRP bars are thus given as = 1.65 based on the experimental findings of the tested beams.**

Keywords: **Lightweight concrete; Beams; GFRP; Crack width; Deflection; Flexural behavior; Bond; Failure; Reinforcement ratio.**

1. INTRODUCTION

Because the de-icing chemicals used corrode steel reinforcement, FRP bars are increasingly being utilized in concrete beams instead of steel bars. The main benefits of FRP bars over traditional steel bars are their high durability (i.e., corrosion resistance) and low strength-to-weight ratio. Over the last 15 years, fiber-reinforced polymer (FRP) has become commercially available as concrete reinforcement. Because there are no well-established standards, a wide range of FRP bars is currently available, ranging from simple smooth and helically deformed bars to bars with exterior features like sand-coating. Most design codes and guides suggest the over-reinforced section design at the ultimate limit state [1], [2]. where concrete crushing is the major mode of failure. In recent years, the concrete industry has made great strides, particularly with the development of lightweight concrete (LWC), which has emerged as a competitive alternative to normal-weight concrete (NWC). LWC can be used to create reinforced concrete (RC) elements (beams, slabs, columns, and foundations) with a lower self-weight and a smaller cross-sectional dimension, saving money in the process because of its lower density .

2. RESEARCH SIGNIFICANCE

The serviceability of LWC beams reinforced with FRP bars has only been the subject of a few investigations. However, studies seem to have examined the cracking behaviour of glass-reinforced polymer (GFRP) bars reinforced lightweight concrete (LWC) beams and calculating the bond-dependent coefficient (kb) values. Additionally, no FRP design standards or guidelines have specifically taken the serviceability of FRP-reinforced LWC (FRP-LWC) members into account. The bond-dependent coefficient kb and cracking behavior control of LWC beam specimens reinforced with FRP bars with varying of concrete cover seem to be the focus of this paper.

As a result, this research has several objectives: (1) to study the cracking behaviour of reinforced LWC beams, (2) to compare the measured deflections and crack widths to those predicted by models in the FRP provisions and literature. The results of this research can be utilized to assess and examine if using GFRP bars in LWC members that are subjected to flexural loads is feasible.

3. EXPERIMENTAL WORK

3.1 Materials

3.1.1 Reinforcing bars

Four representative specimens with different surface texture were tested according to (ASTM D7205, 2011) to assess the tensile properties of the FRP bars. The reference beam was also made of 12mm deformed steel bars. The mechanical properties of the reinforcing bars are summarized in Table (1). The surface layout of GFRP, and steel bars is shown in Figure (1). The GFRP bars during tensile test are shown in figure (2). A stress-strain curve of GFRP and steel bars is shown in figure (3).

TABLE 1: Tensile Properties and Bond Strength of BFRP and Steel Bars

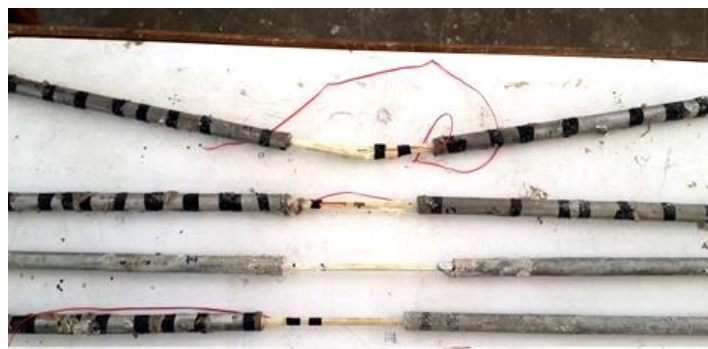| Bar type	Surface texture	Nominal diameter d_b (mm)	Cross sectional area A_f (mm²)	Tensile strength F_{fu} (MPa)	Modules of elasticity E_f (GPa)	Average Rupture Strain ε_{FU} (%)
GFRP bars	Smooth	12	113	675.6	35.68	1.893
Steel	Deformed	12	113	400	200	0.2

Fig. 1: The tested GFRP bars

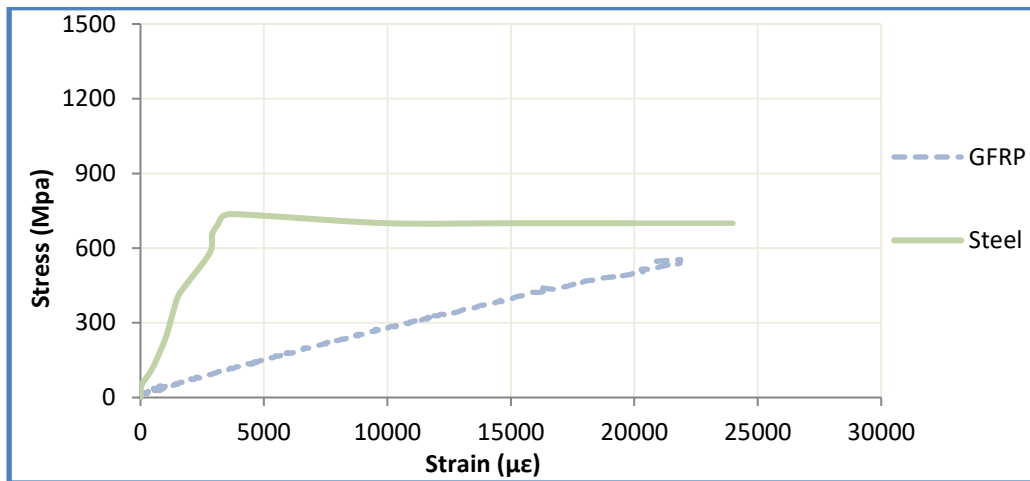**Fig. 2: GFRP bars during the tensile test.**

Fig. 3: The stress-strain curve of used RFT bars

3.1.2 CONCRETE

LWC was utilized to make the specimens used in this experiment (lightweight concrete). Sileous sand and fine, high-quality crushed stone are the main ingredients in both fine and coarse aggregates. All examples were constructed with regular Portland cement. The mixture also included silica fume, basalt fiber, and polystyrene foam. Superplasticizers were employed to make lightweight concrete workable. For concrete quality inspection, three cylinders with a 150 mm diameter and 300 mm length and six standard cubes with dimensions of 150x150x150 mm were made from each batch. The standard cube and cylinder specimen castings for LWC are depicted in Figure (4). After 28 days, concrete cubes were put through a compression test in the lab. The average concrete cubic compressive strength, density and tensile strength of LWC are shown in Table (2).

Fig. 4: Casting the Standard Cubes and Cylinders

TABLE 2: Mechanical properties of LWC cubes

Properties	Denisty kg/m3	Tensile strength (N/mm2)	Compressive Strength (N/mm2)
Value	17.8	1.47	28.3

3.1.3 Beams details and test matrix

Three simply supported LWC beams were constructed and tested under flexure loading until failure, one of which was reinforced with steel bars as a reference beam and the other two with GFR bars. The tested beams were 2000 mm long, 150 mm broad, and 300 mm deep. The beam specimens were strengthened with 8 mm stirrups every 100 mm in the shear spans to prevent bond failure and to minimize the effect of the shear-induced deformation on the mid-span deflection. The beams have a 100 mm overhang length beyond the supports on either side to prevent shear failure. Two 8mm steel bars were used as longitudinal reinforcement for each specimen as shown in Figure (5), The 35mm and 20mm thick clear concrete cover had a thickness.

Fig. 5: the RFT details of tested beams

3.1.4 Specimen fabrication details

Ten lightweight concrete beams were simultaneously made using three wood forms, with the reinforcing cages being cut 20 mm on each end to fit into the 2000 mm long forms. Water was used to moisten the forms so that the beams could be easily released. Concrete casting utilized casting beams and a mechanical vibrator to minimize voids. The wooden forms held the beams up for one day, after which they were all released and allowed to cure for 28 days while being sprinkled with water.

3.1.5 Instrumentation of beam specimen

In Figure (6), instrumentation information is displayed. The deflection along the beam's span was measured using three 0.001 mm accurate linear variable differential transducers (LVDTs), designated D1-D3 (D1 at mid-span and D2 and D3 under the concentrated stresses). Additionally, the crack width was determined, and crack growth was monitored up until test failure. The longitudinal GFRP reinforcing bars' stresses were measured using two electrical-resistance strain gauges that were each 6 mm long (S1-S2). The compressive concrete strains at the mid-span section were measured using an electrical resistance strain gauge that was 60 mm long (C1). Before the test, the beams were painted white to make it simpler to check for cracks and to highlight any already present fissures.

3.2 Test setup and procedure

The simply supported beams were tested in the structural laboratory of the Department of Civil Engineering at Helwan University under monotonic load in four-point bending till failure. An image of the test setup for beam specimens is shown in Figure (7). Until the first crack developed, the beams were visually inspected throughout the testing procedure, at which point the associated load was recorded. The test was terminated after the first three cracks. The change in stiffness of the load-deflection and load-strain relationships, which was based on the cracking load, was also confirmed. During the test, LVDTs for cracking and deflection as well as strain gauges for the concrete and reinforcement were recorded. Table (3) show the test matrix.

4. TEST RESULTS AND DISCUSSION

4.1 Definition of service-load level, cracking moment and cracking pattern

The design standards for FRP-reinforced concrete members are more stringent than those for steel-reinforced concrete members because FRP reinforcement is noncorroding. Four load levels were developed in this experiment to calculate the moment at service condition. For elements exposed to harsh environments (exterior exposure), the moment at service condition is defined by [3] as the moment that corresponds to a crack-width limit of 0.5 mm, and 0.7 mm, for other elements (interior exposure). For the strain in FRP reinforcement, [4] suggests a strain limit of 2000 to control crack width. Through comparison with the service limit for steel, the strain limit of 2000 was identified.

The crack width for FRP reinforced concrete members was restricted to 0.5 mm, while the allowed strain in steel reinforcement under service condition is equivalent to 1200 with a corresponding crack width of 0.3 mm. During the test, the beams were observed visually till the first crack appeared and corresponding load was recorded Including the self-

weight of the beams, the experimental cracking moment (Mcr-exp) of the GFRP-LWC was noted down.Thus, Mcr depends on the concrete's compressive strength as well as the degree of shrinkage restraint. The following equations are used to estimate Mcr;

$$M_{cr} = \frac{F_r * I_g}{y_t} \tag{1}$$

In both [2], and [1], the cracking moment can be calculated as:

$$Mcr = \frac{0.62\lambda\sqrt{F_c'}}{y_t} * Ig \tag{2}$$

where λ = is the reduction factor for concrete density. [2] yielded a better prediction cracking moment than [1] because of the former's smaller modulus of rupture Flexural. Table (4) shows the test results of cracking moment and flexural capacity moment.
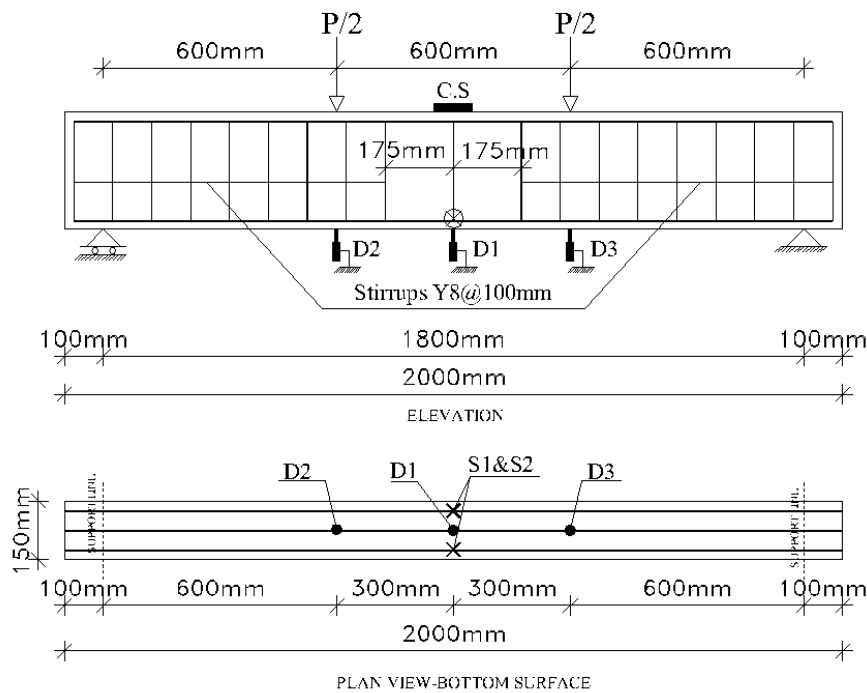

Fig. 6: the instrumentation of the tested beams

4.2 capacity and mode of failure

The concrete beams were made to fail by concrete crushing in compliance with [2], and [1] when the concrete achieved its maximum compressive strain of 0.0030 and 0.0035. Specifically, before the FRP bars' (f_f) maximum tensile stress was reached (f_{fu}), as it is less abrupt, brittle, and catastrophic than the FRP bars' tensile rupture. Previous research [5], and [6] with GFRP-NWC members have reported the same failure sequence. This specimen experienced a shear failure as a result of a mistake made when casting the concrete for the beam. However, because they were under-reinforced when they were planned, as can be seen in figure, the steel-RC beams, which are typical of steel-RC members, failed as a result of the steel bars buckling alongside concrete crushing.

Fig. 7: the test setup of the tested beams

TABLE 3: The test matrix

| Beam (ID) | Reinforcing material | Flexural Reinforcement | | | Concrete cover(mm) | ρf / ρfb | | Axial Stiffness Ef *Af (N) |
		Reinforcement	Surface texture	ρf %		ACI 440.1R-15	CSA S806-12	
B1-3M12-20	Steel	3#12	Deformed	0.825	20	---------	--------	67800
B2-3Y12-SM-20	GFPP	3#12	Smooth	0.825	20	2.6117	2.208	12095.5
B3-3Y12-SM-35	GFPP	3#12	Smooth	0.872	35	2.6117	2.337	12095.52

4.3 Reinforcement and concrete strains

The concrete strain at failure for all of the tested beams was less than the 0.003 or 0.0035 values recommended by design rules and guidelines.

$$M_n = A_f f_f \left(d - \frac{a}{2} \right) + A_f' f_f' \left(\frac{a}{2} - d' \right) \tag{3}$$

Investigations were done into how the GFRP reinforcement ratio affected the LWC beams' normalized moment capacity (Mn/fc′bd^2). Table (4) revealed that increasing concrete cover from 20 mm to 35 mm, while the amount of GFRP bars were constant, decreased the flexural capacity.

4.4 Deflection behavior

The relationship between the applied moment and the mid-span deflection is seen in Fig. (8). All GFRP RC beams originally exhibited linear behaviour until the first flexural crack developed. This was followed by moment-deflection behaviour that was almost linear up until failure. The moment-deflection curve of the steel-LWC beam, in contrast, had a trilinear shape with a yielding plateau. The graph demonstrates how the flexural stiffness of the beams and, consequently, the connection between their moment and deflection, were directly influenced by the quantity of GFRP-bar reinforcement.

TABLE 4: The experimental and predicted results

Beam (ID)	Failure mode	M at conc. Strain =1000 μℰ	Mcr-exp (kN · m)	Mn-exp (kN · m)	Normalized moment capacity	Mcr-exp/Mcr-pred		Mn-exp/Mn-pred
						ACI 440.1R-15	CSA S806-12	ACI 440.1R-15
B1-3M12-20	SY+CC	—	12.5	41.4	—	—	—	—
B2-3Y12-SM-20	CC	9.76	7.41	31.89	0.13	1.14	1.18	0.94
B3-3Y12-SM-35	SF	9.54	7.68	24.60	0.113	1.18	1.22	0.81

4.5 Crack propagation, crack-width prediction, and bond-dependent coefficient Kb

Always starting just at the bottom surface of the beam and extending vertically into the compression zone, the first cracks always developed in the constant moment region of the beams. The cracks grew further away from the zone of constant moment toward the supports as the load increased. Cracks outside the constant-moment area were influenced by flexural and shear pressures, which led the cracks to frequently develop a horizontal component. Some longitudinal cracks at the level of the reinforcement appeared between two cracks when the beam's nominal capacity was being approached by high loads, but they had no impact on the failure mode. Crack-width equations According to, and [3], [4]Canada Research Network model Eq. (4), and Eq. (5) must take the following into consideration when calculating the crack-width of flexural elements reinforced with longitudinal FRP bars:

$$W_{cr} = \frac{2f_{fs}}{E_f}\frac{h_2}{h_1}k_b\sqrt{d_c^2 + \left(s_{m_{ax}} / 2\right)^2} \qquad (4)$$

$$w = 2.2k_b \frac{f_f}{E_f}\frac{h_2}{h_1}(\ dC \ A)1/3 \qquad (5)$$

[2] ACI 440. 1R-15equation:

$$s_{m_{ax}} = 1.15 \frac{E_f}{f_{fs}}\frac{W_{cr}}{k_b} - 2.5c_c \leq 0.92 \frac{E_f}{f_{fs}}\frac{W_{cr}}{k_b} \qquad (6)$$
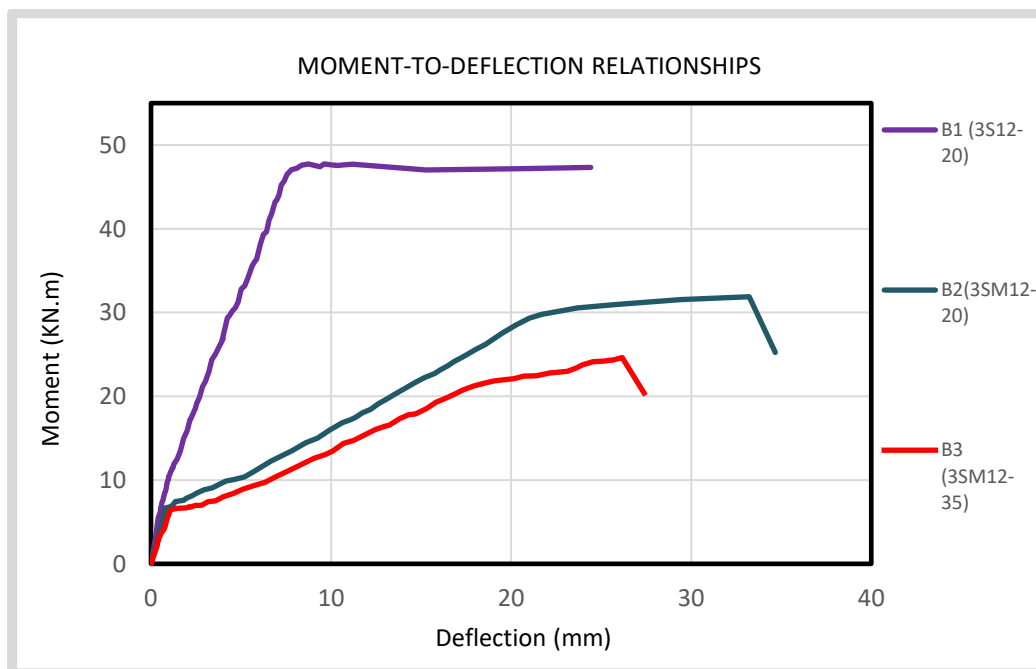

Fig 8: Moment-mid-span deflection relationships

It appears that smooth FRP bars in LWC beams work effectively with a kb value of 1.6. To evaluate and enhance the present kb values in FRP standards, future experimental and theoretical studies with more measurements and calculations are suggested. Table (5) shows Average predicted Kb values for (Smooth) GFRP bars.

TABLE 5: Average predicted Kb values for (Smooth) GFRP bars.

Beam (ID)	ACI 440. 1R-15		CSA S6-19		ISIS (2007)	
(Kb) at	0.3Mn	2000µℇ	0.3Mn	2000µℇ	0.3Mn	2000µℇ
B2-3Y12-SM-20	1.57	3.69	1.69	3.90	1.25	2.88
B3-3Y12-SM-35	1.73	2.21	1.80	2.28	1.34	1.70
(Kb) Average	1.65	2.95	1.75	3.09	1.30	2.29

5. SUMMARY AND CONCLUSION

This paper reviews an experimental study that investigated the flexural behavior, cracking capability, and bond-dependent (Kb) properties of beams made of lightweight concrete. Three lightweight concrete beams, each 150 mm wide, 300 mm deep, and 2000 mm long, were developed and tested in four-point bending over an 1800 mm clear span until they failed. One of these beams served as a reference beam and was reinforced with steel bars. The other beams were reinforced with GFR bars. Reinforcement type (steel bars and GFRP bars), and concrete cover were the test parameters. The following conclusions are reached in the context of the test results and analysis presented here:

1) Up until failure, the GFRP-RC beams exhibited normal bilinear strain and deflection characteristics. The reinforcing ratio had no effect on the pre-cracking reaction and cracking loads of any of the beams because it is determined by the gross concrete section. However, the reinforcement ratio was correlated with either an increase in stiffness or a decrease in reinforcement strains following cracking. With a larger reinforcement ratio, stiffness and strain at the same load level rise. Low reinforcement ratio GFRP-RC beams showed sharp increases in stresses and deflection at cracking. The stiffness and location of the neutral axis of the cracked section reflect the wider and deeper cracks caused by the abrupt increase in stresses. However, increasing the reinforcement ratio increased the amount of energy absorbed at the first crack, which improved the behavior because it controls the initial increase in strain and crack width.

2) The general behavior of the GFRP-RC beams was significantly impacted by the axial stiffness of the flexural reinforcement (EfAf). The efficiency increases with increasing axial stiffness (lower deflection, lower strain, and lowered crack width at the same load level). It is expected that beams with the same axial stiffness of reinforcement will behave similarly.

3) According to the experiment results, the FRP bars with a sand-coated surface, smooth surface, and GFRP bars with a ribbed surface all had significantly different values for kb. For the smooth 1.6.

4) It is recommended to continue this study with additional experimental effort, taking into account more samples for each group to test for each test parameter, and to assess the recommended kb values that have been introduced in this study.

REFERENCES

[1] CAN/CSA S806-12. (2012). Design and Construction of Building Components with Fibre Reinforced Polymers. In Canadian Standards Association. Rexdale, ON, Canada.

[2] ACI 440.1R-15. (2015). In A. C. ACI Committee 440, Guide for the Design and Construction of Concrete Reinforced with FRP Bars. Farmington Hills, MI.

[3] CSA S6. (2019). Canadian highway bridge design code. . Rexdale, Ontario, Canada.: Canadian Standards Association (CSA).

[4] ISIS . (2007). Canada Research Network, Reinforced Concrete Structures with Fibre-Reinforced Polymers,. Winnipeg, MB, Canada,: ISIS Manual No. 3, University of Manitoba,.

[5] El-Nemr, A., E. A. Ahmed, C. Barris, and B. Benmokrane. (2016). "Bond-dependent coefficient of glass-and carbon-FRP bars in normaland high-strength concretes.". Constr. Build. Mater. 113: 77–89. Retrieved from https://doi.org/ 10.1016/j.conbuildmat.2016.03.005.

[6] F. Elgabbas, P. Vincent, E.A. Ahmed, B. Benmokrane. (2016). Experimental testing of basalt fiber-reinforced polymer bars in concrete beams. Compos. B Eng. 91, 205–218.

[7] ASTM D7205. (2011). Tensile Properties of Fiber Reinforced Polymer Matrix Composite Bars. West Conshohocken, PA: ASTM International.